
PECULIARITIES OF MEDIUM PARAMETER DYNAMICS AND COSMIC RAY DENSITY IN STRONG FORBUSH DECREASES ASSOCIATED WITH MAGNETIC CLOUDS

A.S. Petukhova 

*Yu.G. Shafer Institute of Cosmophysical Research
and Aeronomy of SB RAS,
Yakutsk, Russia, petukhova@ikfia.ysn.ru*

I.S. Petukhov 

*Yu.G. Shafer Institute of Cosmophysical Research
and Aeronomy of SB RAS,
Yakutsk, Russia, i_van@ikfia.ysn.ru*

S.I. Petukhov 

*Yu.G. Shafer Institute of Cosmophysical Research
and Aeronomy of SB RAS,
Yakutsk, Russia, petukhov@ikfia.ysn.ru*

I.S. Gotovtsev

*Yu.G. Shafer Institute of Cosmophysical Research
and Aeronomy of SB RAS,
Yakutsk, Russia, i_gotovtsev@mail.ru*

Abstract. Diffusion and electromagnetic mechanisms determine the formation of sporadic Forbush decreases (FDs). The diffusion mechanism affects the FD amplitude (A_{FD}) in the turbulent layer, and the part of the coronal mass ejection (CME) preceding the magnetic cloud, and its efficiency depends on the level of magnetic field turbulence. The electromagnetic mechanism works in a magnetic cloud, and its efficiency depends on the intensity of regular magnetic and electric fields. We analyze solar wind parameters and cosmic ray density, using the superposed epoch analysis. In 1996–2006, 23 strong FDs ($A_{FD} > 5\%$) were detected. The average amplitude of 7% is equally formed by both mechanisms. The events can be divided into 2 groups depending on the contribution of the mechanisms to A_{FD} . Group 1 includes the strongest FDs ($A_{FD1} = 8.5\%$), formed by both diffusion and electromagnetic mecha-

nisms. The diffusion mechanism forms $0.26A_{FD1}$, and the electromagnetic mechanism is responsible for $0.74A_{FD1}$. In group 2, the amplitude $A_{FD2} = 5.7\%$, the diffusion mechanism forms $0.79A_{FD2}$ of the amplitude; and the electromagnetic one, $0.21A_{FD2}$. The spatial distributions of the mean values of the medium parameters in the region of disturbances in the groups differ. This difference can be explained by the fact that A_{FD} in groups 1 and 2 are formed in the central and peripheral parts of CME respectively.

Keywords: cosmic rays, coronal mass ejection, Forbush decrease, solar wind, interplanetary magnetic field, shock, magnetic cloud.

INTRODUCTION

Coronal mass ejections (CMEs) carry plasma out of the solar atmosphere into interplanetary space. In some cases, a large-scale loop with a helical magnetic field, called a magnetic cloud (MC), is carried away along with the substance. At a distance of 1 AU from the Sun, about 1/3 of CMEs show evidence of MC [Richardson, Cane, 2011]. A shock front precedes CME moving at a super-Alfvén velocity relative to the solar wind. The region between the shock front and the leading edge of CME is called the turbulent layer. In this region, the energy density of regular (smoothly varying in time and space) and turbulent (sharply varying in time and space) magnetic fields increases significantly. The increase in the energy of the regular and turbulent magnetic fields is caused by the impact of the shock front and CME. CMEs are the most powerful solar phenomena since they strongly affect the properties of solar wind plasma, geomagnetic activity [Kilpua et al., 2017], and space-time distribution of cosmic rays (CRs) [Belov et al., 2014]. The important role of solar atmosphere processes in forming space weather maintains the interest in CMEs in heliospheric research. Results of local spacecraft measurements and their extrapolation to larger

scales are usually used to determine the shape and properties of CMEs. Nonetheless, the possibility of identifying the large-scale properties of CMEs only from local measurements is limited. Due to their high mobility, CRs contain information that may not be available in local measurements. The result of the CME impact on CRs, expressed as a change in the counting rate of ground-based CR detectors, is called a Forbush decrease (FD). For the first time, FDs were discovered by Forbush [1937] and Hess, Demmelmair [1937] using ionization chambers. For more detailed information on the observed properties of FDs, see [Belov, 2009].

FD is an accurate identifier of CMEs. Statistical study by Richardson, Cane [2011] has shown that FDs accompanied 80% of 300 CME events. There is no generally accepted estimate of the shock front, turbulent layer, and CME contributions to the FD amplitude. There are different estimates of the MC contribution: a) no contribution [Reames et al., 2009]; b) insignificant contribution [Badruddin et al., 1991]; c) contribution equal to the turbulent layer and CME contributions [Richardson, Cane, 2011]. The difference in the estimates can be explained by a large number of weak FDs, a change in the FD amplitude in individual events, and a different number of events analyzed by the authors. For

example, Belov et al. [2015] have found that the FD amplitude in MC was less than 0.5 % in half of the 99 events observed in 1996–2009.

In this paper, we assume that the FD amplitude is formed by diffusion and electromagnetic mechanisms. The contribution of various mechanisms to the FD amplitude is assessed from the results of the analysis of selected events. The paper is organized as follows. Section 1 presents data and analysis, as well as information on diffusion, electromagnetic mechanisms, and non-diffusion propagation of particles during FD formation. Section 2 assesses the contribution of the mechanisms to the amplitude of strong FD. Section 3 draws conclusions from the results of the study.

1. DIFFUSION AND ELECTROMAGNETIC MECHANISMS OF FD FORMATION

1.1. Data and analysis

We employ 1-hour data on solar wind and interplanetary magnetic field parameters: solar wind velocity V [km/s]; longitude of the total flux φ_v [degree] (changes in the positive/negative direction from zero as the flux changes direction from the $-X_{GSE}$ axis to the $+Y_{GSE}/-Y_{GSE}$ axis); latitude of the total flux θ_v [degree] (changes in the positive/negative direction from zero as the flux changes direction from $X_{GSE}-Y_{GSE}$ to $+Z_{GSE}/-Z_{GSE}$); magnetic field components B_x, B_y, B_z [nT] in the GSE coordinate system and magnetic field strength modulus $|B|$ [nT]; the standard deviation of the magnetic field strength vector σB [nT] [<https://omniweb.gsfc.nasa.gov/form/dx1.html>].

The analysis uses the electric field strength E [mV/m] whose absolute value is calculated from its components E_x, E_y, E_z [mV/m]. The components, in turn, are determined by the vector product of the flux velocity and the magnetic field strength $\mathbf{E} = -\mathbf{V} \times \mathbf{B}$. Cartesian components of the flux vector in GSE coordinates can be derived from velocity and angles as $V_x = -V \cos(\theta_v) \cos(\varphi_v)$, $V_y = +V \cos(\theta_v) \sin(\varphi_v)$, $V_z = +V \sin(\theta_v)$, the flux angle φ_v OMNI is opposite to the GSE angle φ_v .

We also use 1-hour data on the CR density Δn [%] obtained by the IZMIRAN Cosmic Ray Group [<http://spaceweather.izmiran.ru/eng/dbs.html>] with the global survey method [Belov et al., 2018]. The superposed epoch method was employed to analyze the CR density, the solar wind velocity, σB , as well as magnetic and electric field strengths. We apply two variants of zero hour: 1) time of shock front arrival at Earth; 2) time of MC arrival at Earth. The duration of the event is related to the zero hour. The analyzed interval is 72 hrs before and 216 hrs after the zero hour. The shock front and MC arrival times correlate with the CME catalog compiled by Richardson and Cane [<http://www.srl.caltech.edu/ACE/ASC/DATA/level3/icmetable2.htm>].

1.2. Mechanisms of FD formation

CME moving in interplanetary space causes the CR intensity to change. A decrease in the intensity accompanied 80 % of 300 CMEs recorded in 1995–2009; no changes occurred in 10 % of the events, and an increase was observed in 10 % of the events [Richardson, Cane, 2011]. A minimum intensity was seen inside CMEs in 90 % of the events. A_{FD} is a relative value of maximum intensity decrease (in %). Statistical analysis has shown that the diffusion mechanism causes a decrease in intensity due to a decrease in particle diffusion in the turbulent layer [Lockwood et al., 1991] or due to perpendicular diffusion at the outer boundary of MC [Cane et al., 1995]. Theoretical definitions of FD characteristics (as a rule, the CR density) are based on solving the particle transport equation in the diffusion approximation for different disturbance velocities and diffusion coefficient [Krymskii et al., 1974], as well as with allowance for the drift [Kadokura, Nishida, 1986]. Luo et al. [2017] have calculated the FD characteristics, using a three-dimensional nonstationary model and taking into account the tilt angle of the heliospheric current sheet.

The diffusion mechanism is also used in calculating the FD characteristics in MC. CRs are thought to fill the MC through perpendicular diffusion [Cane et al., 1995]. In all these models, the diffusion coefficient is a free parameter.

Non-diffusion propagation of particles driven by a helical field has recently attracted the attention of researchers. Krittinatham, Ruffolo [2009] have calculated velocities of the particle drift caused by the magnetic field helicity and gradient in a helical field. They found that CRs can be trapped for a long time. The drifts should be attended with the formation of unidirectional anisotropy with a direction determined by a poloidal field. For the April 13, 2013 event, Tortermun et al. [2018] have established that there was a strong unidirectional flux inside the closed helical field, as predicted by their model.

Benella et al. [2020] have examined the role the MC magnetic structure plays in forming FDs. They estimated the FD amplitude and its time profile in MC, obtained by reconstructing the magnetic field geometry with the Grad–Shafranov method and by calculating particle trajectories. Model calculations allow us to study the MC effect on CR propagation. Comparing the model outputs with observations has revealed that the drifts play an important role in forming FDs, and the CR diffusion makes a small contribution.

Laitinen, Dalla [2021] have examined the transition of CRs from the open interplanetary magnetic field to a region filled with isolated field lines. They found that CRs can penetrate through an X-point region between isolated and open magnetic field lines. The transition is fast and consistent with the simple radial diffusion model in which particles enter through the boundary of an isolated magnetic field.

Petukhova et al. [2019] have proposed an electromagnetic mechanism for the FD formation in MC. The mechanism involves two processes: a) CR energy loss in an induction electric field of moving MC; b) accumulation of CR energy losses due to quasi-trapping in a

helical magnetic field. The CR distribution function and its three moments (CR density, vector and tensor anisotropies) are determined by solving the Boltzmann kinetic equation without particle scattering. Relationships between the distribution function and its three moments, used to compare calculation results with measurements, have been obtained by Petukhova et al. [2019]. The magnetic field structure in MC is specified at the initial moment in the form of a torus, and then changes over time according to the freezing-in condition [Petukhova, Petukhov, 2019]. It has been found that the FD characteristics depend on the following MC parameters:

- magnetic field strength and its spiral structure; electric field strength; plasma stream velocity and velocity gradient; magnetic configuration (MC type according to [Bothmer, Schwenn, 1998]);
- geometrical dimensions (angular width in longitude and cross-section dimension);
- paths along which Earth crosses MC.

Comparing the calculation results with the measurements for two events shows that [Petukhova et al., 2020]:

- a) FD amplitudes quantitatively correspond;
- b) CR density is described by a parabolic function depending on the distance to the MC center;
- c) vector anisotropy changes abruptly when crossing the MC boundary (it is higher in MC);
- d) north-south vector anisotropy component changes sign near the MC center;
- e) ecliptic anisotropy component rotates in MC.

The above-mentioned model of the FD characteristics, formed by the electromagnetic mechanism, generally represents the observed CR density and vector anisotropy [Abunin et al., 2013; Belov et al., 2015]. The FD amplitude is shown to be independent of the MC type, whereas the anisotropy vector strongly depends on it. There are no free parameters in the presented model of FD formation in MC.

2. SUPERPOSED EPOCH METHOD

The FD amplitude consists of two parts. One part (A_{DM}) is formed by the diffusion mechanism (DM) in the turbulent layer and in the part of CME preceding MC; the second part (A_{EM}) is formed by the electromagnetic mechanism (EM) in MC: $A_{DM}+A_{EM}=A_{FD}$. The ratio between these two parts determines the relative contribution of the FD mechanisms. We use the superposed epoch method to analyze 1-hour data on CR density, solar wind velocity, magnetic and electric field strengths, σV . The MC boundary divides the areas of the FD formation mechanisms; therefore, we take the time when Earth crosses the MC boundary as zero hour. We analyze only strong FDs. The following criteria are adopted for the selected events: $A_{FD}>5\%$; there is a shock wave, CME with MC; solar wind parameters and magnetic field data are available in the OMNI database; time of commencement of a disturbance, CME and MC boundaries are available in the CME catalog; CR characteristics are available in the database created by the IZMIRAN Cosmic Ray Group.

According to the above criteria, we have identified 23 FDs for the period 1996–2006. The July 22, 2004 event was excluded from the analysis because the leading edge of MC was detected before the CME. The events are listed in Table. Dates of the events have been

Strong FDs in 1996–2006

№	Group 1	Group 2
1	July 13, 2000	May 01, 1998
2	July 15, 2000	September 24, 1998
3	October 28, 2000	November 08, 1998
4	November 06, 2000	February 18, 1999
5	April 04, 2001	April 11, 2001
6	October 29, 2003	April 28, 2001
7	November 20, 2003	November 24, 2001
8	July 26, 2004	March 18, 2002
9	November 09, 2004	April 17, 2002
10	May 15, 2005	May 23, 2002
11		July 24, 2004
12		November 07, 2004
13		December 14, 2006

taken from the catalog compiled by Richardson and Cane. The commencement time coincides with the storm sudden commencement (usually associated with the arrival of a shock front at Earth). OMNI data gaps were filled with linearly interpolated values. In the analysis, we restricted ourselves to the events recorded during solar cycle 23 since there are MC boundaries for them in the catalog by Richardson and Cane. There was an attempt to expand the sample to the events of cycle 24, but MC boundaries for them are not given in this catalog. We had to omit a similar WIND catalog, as the time of recording of magnetic obstacle boundaries indicated is inconsistent with the data from the catalog by Richardson and Cane. Presumably, the times in the WIND catalog correspond to CME boundaries rather than to MC ones.

The upper panel of Figure 1 shows the average amplitude of strong FD ($A_{FD}=7\%$), which consists of two parts formed by DM and EM respectively: $A_{DM}=0.5 A_{FD}=3.5\%$ and $A_{EM}=0.5 A_{FD}=3.5\%$.

Strong FDs can be divided into two groups depending on the ratio of A_{DM} to A_{EM} . Figure 2 presents the CR density dynamics obtained by the global survey method, developed at IZMIRAN, in two events. Vertical lines indicate a shock front (thick line), CME boundaries (thin lines), and the MC boundaries (dashed lines). Figure 2 illustrates how the events were grouped. In Figure 2, *a* (the November 9, 2004 event), the CR density in the turbulent layer decreases by 1%; and in MC, by 7% ($A_{EM}>A_{DM}$), so this event belongs to group 1. In Figure 2, *b* (the April 28, 2001 event) in the turbulent layer, the CR density decreases by 7.2%; and in MC, by 0.1% ($A_{EM}<A_{DM}$), hence this event is assigned to group 2.

Table lists strong FDs occurring during 1996–2006, divided into two groups: 10 FDs are in group 1; 13 FDs are in group 2.

Figures 3, 4 present the results of the analysis of the two groups of strong FDs obtained by the superposed epoch method with two zero hour variants. Spatial distributions of the relative CR density and the solar wind parameters are shown when the times of arrival of the shock front (Figure 3) and MC (Figure 4) at Earth are used as the zero hour. Red, green, and black lines represent the parameters of groups 1, 2, and all events respectively. The vertical dashed line marks the zero hour.

Figure 3, *b–e* suggests that the spatial distributions of the solar wind parameters relative to the shock front are similar, with maximum values of the parameters in the

group 1 events being larger. The magnetic field turbulence, represented by the parameter σB , coincides both in spatial distribution and in σB_{\max} in the events of these groups (Figure 3, *e*). Figure 3, *a* shows that the recovery time of the FDs from group 2 is noticeably longer. It is known that the east-west asymmetry is observed in sporadic FDs: the amplitudes and recovery times in eastern FDs are greater than in western FDs. Accordingly, we can assume that

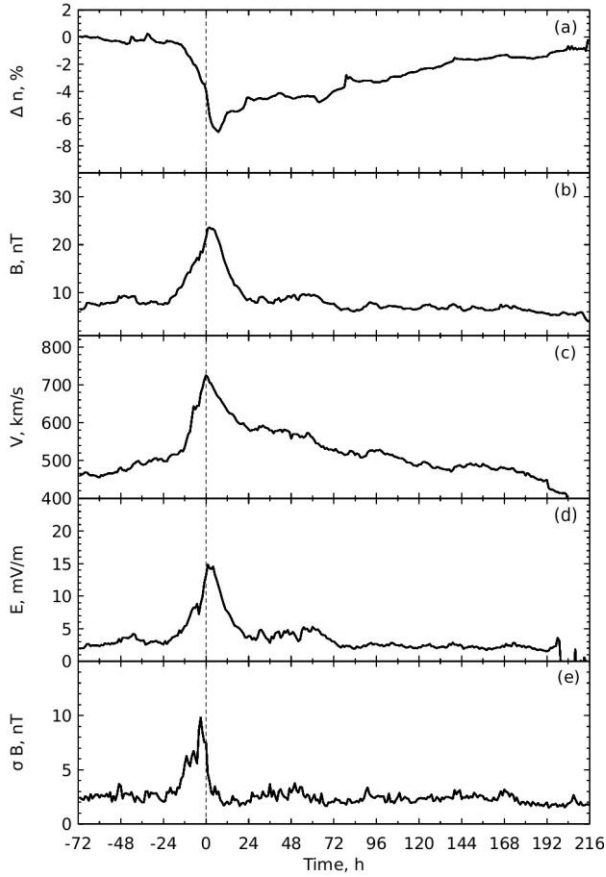


Figure 1. Mean values of CR and solar wind parameters: CR density (*a*); magnetic field modulus (*b*); solar wind velocity (*c*); electric field modulus (*d*); standard deviation of the magnetic field vector (*e*). Zero hour corresponds to the time when Earth crosses the MC boundary

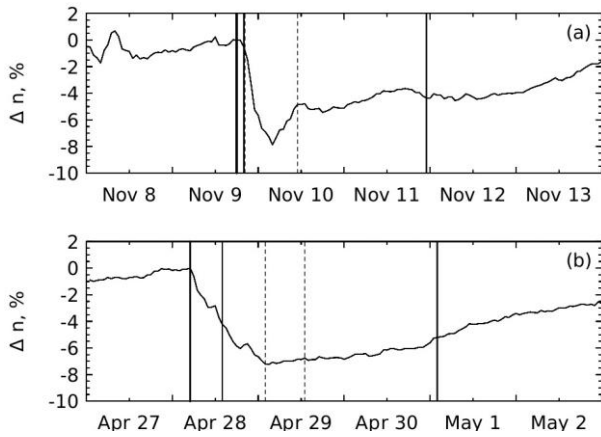


Figure 2. CR density as a function of time for the events of November 9, 2004 (*a*) and April 28, 2001 (*b*). Vertical lines indicate a shock wave front (thick lines), CME boundaries (thin lines), and MC boundaries (dashed lines)

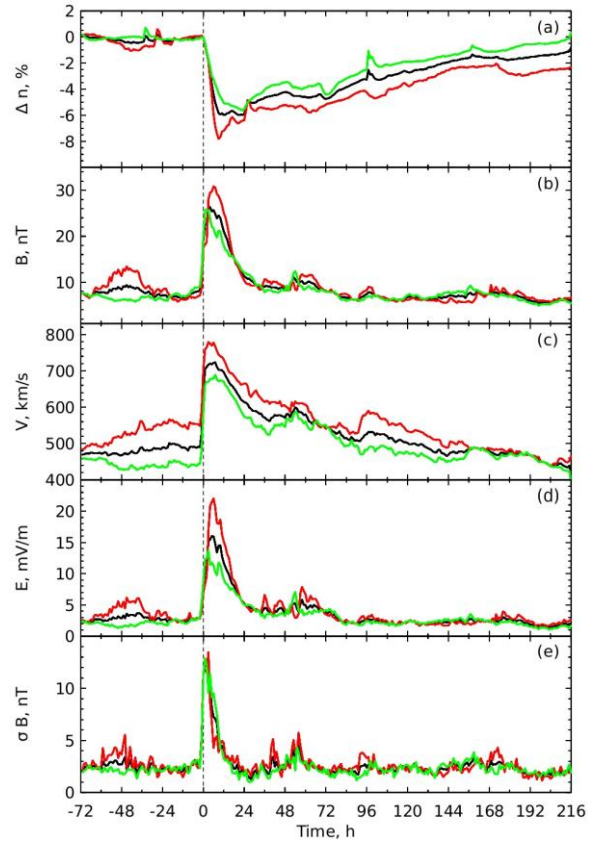


Figure 3. The same as in Figure 1 for the group 1 (red curves) and 2 (green curves) events and for all events (black curves). Zero hour (vertical dashed line) corresponds to the arrival of the shock front at Earth

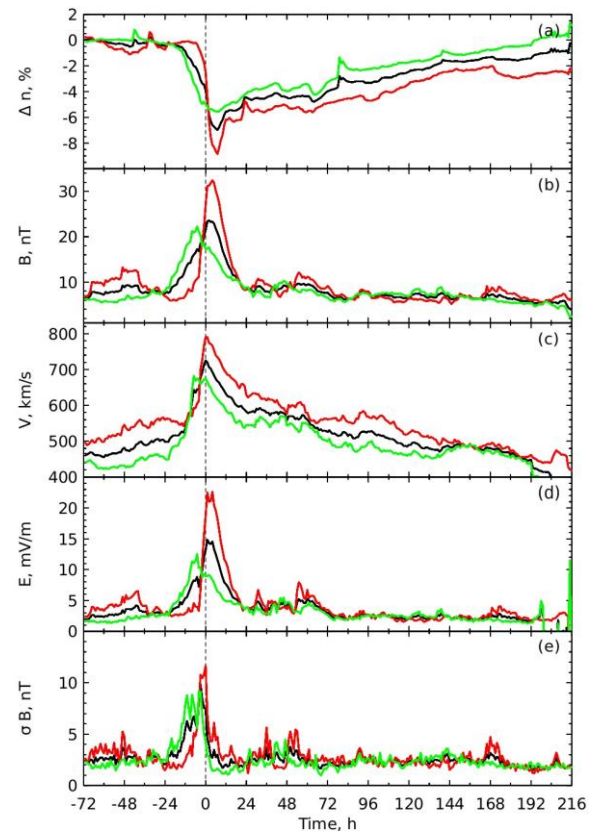


Figure 4. The same as in Figure 3. Zero hour corresponds to the arrival of MC at Earth

FDs from groups 1 and 2 were formed when Earth crossed the frontal and eastern parts of CME respectively. There are no FDs, formed when Earth crossed the western part of the CME, in the sample since they do not meet the selection criterion $A_{FD} > 5\%$.

Figure 4, *b–e* illustrates the difference between the groups of spatial distributions of solar wind parameters and their maximum values relative to the front boundary of MC. The figures suggest that the time interval (size of the region) between the commencement of the disturbance (shock front) and the front boundary of MC in the group 2 events is longer. Figure 4, *e* shows that the spatial distribution and the magnetic turbulence level in the groups differ. The spatial distribution of CR density in the region ahead of the MC boundary in the groups (Figure 4, *a*) matches the turbulence distribution (Figure 4, *e*).

Figure 4, *a* demonstrates the difference between FD amplitudes in groups 1 and 2: $A_{FD1} = 8.5\%$ and $A_{FD2} = 5.7\%$. The contributions of the mechanisms in the groups vary greatly: $A_{DM1} = 0.26A_{FD1} = 2.2\%$, $A_{EM1} = 0.74A_{FD1} = 6.3\%$, $A_{DM2} = 0.79A_{FD2} = 4.5\%$, $A_{EM2} = 0.21A_{FD2} = 1.2\%$. The formation of the two groups of strong FDs differing in the spatial distribution of solar wind parameters, maximum values of the parameters, the recovery time of the decreases, and the contributions of the mechanisms to the FD amplitude results from the observed east-west asymmetry of FDs. The asymmetry is attributed to the difference between the contributions of the electromagnetic and diffusion mechanisms to the FD amplitude in different CME parts. The diffusion mechanism manifests itself in all the sampling events since there is a shock front and hence a turbulent layer in all the events. The electromagnetic mechanism reveals itself only in the frontal part of CME (group 1). The EM inefficiency in the peripheral part of MC (group 2) can be explained by the absence of a helical magnetic field [Owens, 2016] — the cause of the quasi-trapping of particles.

CONCLUSION

Diffusion and electromagnetic mechanisms are involved in the formation of sporadic FDs. The diffusion mechanism is effective outside the magnetic cloud, where there is an increased level of magnetic field turbulence. The electromagnetic mechanism works in the vicinity of the helical magnetic field of MC.

The results of the analysis of strong FDs recorded in 1996–2006 and satisfying the accepted selection criteria show that the average FD amplitude is 7%; the contributions of the diffusion and electromagnetic mechanisms coincide $A_{DM} = 0.5A_{FD} = 3.5\%$ and $A_{EM} = 0.5A_{FD} = 3.5\%$.

Strong FDs can be divided into two groups depending on the ratio between the contributions of the diffusion and electromagnetic mechanisms: $A_{EM} > A_{DM}$ in group 1 and $A_{EM} < A_{DM}$ in group 2. Group 1 includes the strongest FDs formed by the diffusion and electromagnetic mechanisms. The average FD amplitude $A_{FD1} = 8.5\%$, including the contributions of the diffusion mechanism $A_{DM1} = 0.26A_{FD1} = 2.2\%$ and the electromagnetic mechanism $A_{EM1} = 0.74A_{FD1} = 6.3\%$. The average FD amplitude in group 2 $A_{FD2} = 5.7\%$, including the contributions of the diffusion mechanism $A_{DM2} = 0.79A_{FD2} = 4.5\%$ and the elec-

tromagnetic mechanism $A_{EM2} = 0.21A_{FD2} = 1.2\%$.

The two FD groups may be formed as a result of frontal and peripheral crossings of CME by Earth and may be due to the inefficiency of the electromagnetic mechanism because of the absence of a helical magnetic field.

The work was financially supported by the Ministry of Science and Higher Education of the Russian Federation (Project FWRS-2021-0012). We express our gratitude to IZMIRAN for the FD database [<http://spaceweather.izmiran.ru/eng/dbs.html>], and also thank the teams who created the databases OmniWeb [<https://omniweb.gsfc.nasa.gov/form/dx1.html>] and NMDB [<https://www.nmdb.eu>] for providing data, and I.G. Richardson and H.V. Cane for compiling the catalog of near-Earth interplanetary CMEs [<http://www.srl.caltech.edu/ACE/ASC/DATA/level3/icmetable2.htm>].

REFERENCES

- Abunin A., Abunina M., Belov A., Eroshenko E., Oleneva V., Yanke V., Mavromichalaki H., Papaioannou A. The impact of magnetic clouds on the density and the first harmonic of the cosmic ray anisotropy. *ICRC*. 2013, vol. 33, 1618.
- Badruddin B., Venkatesan D., Zhu B.Y. Study and effect of magnetic clouds on the transient modulation of cosmic-ray intensity. *Solar Phys.* 1991, vol. 134, no. 1, pp. 203–209. DOI: [10.1007/BF00148748](https://doi.org/10.1007/BF00148748).
- Belov A.V. Forbush effects and their connection with solar, interplanetary and geomagnetic phenomena. *Universal Heliophysical Processes*. 2009, vol. 257, pp. 43–450. DOI: [10.1017/S1743921309029676](https://doi.org/10.1017/S1743921309029676).
- Belov A., Abunin A., Abunina M., Eroshenko E., Oleneva V., Yanke V., Papaioannou A., Mavromichalaki H., Gopalswamy N., Yashiro S. Coronal mass ejections and non-recurrent Forbush decreases. *Solar Phys.* 2014, vol. 289, no. 10, pp. 394–3960. DOI: [10.1007/s11207-014-0534-6](https://doi.org/10.1007/s11207-014-0534-6).
- Belov A., Abunin A., Abunina M., Eroshenko E., Oleneva V., Yanke V., Papaioannou A., Mavromichalaki H. Galactic cosmic ray density variations in magnetic clouds. *Solar Phys.* 2015, vol. 290, no. 5, pp. 1429–1444. DOI: [10.1007/s11207-015-0678-z](https://doi.org/10.1007/s11207-015-0678-z).
- Belov A., Eroshenko E., Yanke V., Oleneva V., Abunin A., Abunina M., Papaioannou A., Mavromichalaki H. The global survey method applied to ground-level cosmic ray measurements. *Solar Phys.* 2018, vol. 293, no. 4, 68. DOI: [10.1007/s11207-018-1277-6](https://doi.org/10.1007/s11207-018-1277-6).
- Benella S., Laurenza M., Vainio R., Grimani C., Consolini G., Hu Q., Afanasiev A. A new method to model magnetic cloud-driven Forbush decreases: The 2016 August 2 event. *Astrophys. J.* 2020, vol. 901, no. 1, 21. DOI: [10.3847/1538-4357/abac59](https://doi.org/10.3847/1538-4357/abac59).
- Bothmer V., Schwenn R. The structure and origin of magnetic clouds in the solar wind. *Ann. Geophys.* 1998, vol. 16, no. 1, pp. 1–24. DOI: [10.1007/s00585-997-0001-x](https://doi.org/10.1007/s00585-997-0001-x).
- Cane H.V., Richardson I.G., Wibberenz G. The response of energetic particles to the presence of ejecta material. *International Cosmic Ray Conference*. 1995, vol. 4, p. 377.
- Forbush S.E. On the effects in cosmic-ray intensity observed during the recent magnetic storm. *Physical Review*. 1937, vol. 51, no. 12, pp. 1108–1109. DOI: [10.1103/PhysRev.51.1108.3](https://doi.org/10.1103/PhysRev.51.1108.3).
- Hess V. F., Demmelmair A. World-wide effect in cosmic ray intensity, as observed during a recent magnetic storm. *Nature*. 1937, vol. 140, no. 3538, pp. 316–317. DOI: [10.1038/140316a0](https://doi.org/10.1038/140316a0).
- Kadokura A., Nishida A. Two-dimensional numerical modeling of the cosmic ray storm. *J. Geophys. Res.* 1986, vol. 91, no. A1, pp. 13–30. DOI: [10.1029/JA091iA01p00013](https://doi.org/10.1029/JA091iA01p00013).
- Kilpua E., Koskinen H.E.J., Pulkkinen T.I. Coronal mass ejections and their sheath regions in interplanetary space. *Liv-*

ing *Reviews in Solar Physics*. 2017, vol. 14, no. 1, 5. DOI: [10.1007/s41116-017-0009-6](https://doi.org/10.1007/s41116-017-0009-6).

Krittinatham W., Ruffolo D. Drift orbits of energetic particles in an interplanetary magnetic flux rope. *Astrophys. J.* 2009, vol. 704, no. 1, pp. 831–841. DOI: [10.1088/0004-637X/704/1/831](https://doi.org/10.1088/0004-637X/704/1/831).

Krymskii G.F., Transkii I.A., Elshin E.K. Piston shock waves in the interplanetary medium and Forbush effects. *Geomagnetizm i Aeronomiya* [Geomagnetism and Aeronomy]. 1974, vol. 14, no. 3, pp. 407–410. (In Russian).

Laitinen T., Dalla S. Cosmic ray access from external field lines to an ICME fluxrope. *43rd COSPAR Scientific Assembly. Held 28 January – 4 February*. 2021, vol. 43, 866.

Lockwood J.A., Webber W.R., Debrunner H. Forbush decreases and interplanetary magnetic field disturbances: Association with magnetic clouds. *J. Geophys. Res.* 1991, vol. 96, no. A7, pp. 11587–11604. DOI: [10.1029/91JA01012](https://doi.org/10.1029/91JA01012).

Luo X., Potgieter M.S., Zhang M., Feng X. A numerical study of Forbush decreases with a 3D cosmic-ray modulation model based on an SDE approach. *Astrophys. J.* 2017, vol. 839, no. 1, 53. DOI: [10.3847/1538-4357/aa6974](https://doi.org/10.3847/1538-4357/aa6974).

Owens M.J. Do the legs of magnetic clouds contain twisted flux-rope magnetic fields? *Astrophys. J.* 2016, vol. 818, no. 2, pp. 1–5. DOI: [10.3847/0004-637X/818/2/197](https://doi.org/10.3847/0004-637X/818/2/197).

Petukhova A., Petukhov S. Toroidal models of magnetic field with twisted structure. *Solar-Terr. Phys.* 2019, vol. 5, no. 2, pp. 69–75. DOI: [10.12737/stp-52201910](https://doi.org/10.12737/stp-52201910).

Petukhova A.S., Petukhov I.S., Petukhov S.I. Theory of the formation of Forbush decrease in a magnetic cloud: Dependence of Forbush decrease characteristics on magnetic cloud parameters. *Astrophys. J.* 2019, vol. 880, no. 1, p. 17. DOI: [10.3847/1538-4357/ab2889](https://doi.org/10.3847/1538-4357/ab2889).

Petukhova A.S., Petukhov I.S., Petukhov S.I. Forbush decrease characteristics in a magnetic cloud. *Space Weather*. 2020, vol. 18, no. 12, e02616. DOI: [10.1029/2020SW002616](https://doi.org/10.1029/2020SW002616).

Reames D.V., Kahler S.W., Tylka A.J. Anomalous cosmic rays as probes of magnetic clouds. *Astrophys. J.* 2009, vol. 700, no. 2, pp. L196–L199. DOI: [10.1088/0004-637X/700/2/L196](https://doi.org/10.1088/0004-637X/700/2/L196).

Richardson I.G., Cane H.V. Galactic cosmic ray intensity response to interplanetary coronal mass ejections/magnetic clouds in 1995–2009. *Solar Phys.* 2011, vol. 270, no. 2, pp. 609–627. DOI: [10.1007/s11207-011-9774-x](https://doi.org/10.1007/s11207-011-9774-x).

Tortermun U., Ruffolo D., Bieber J.W. Galactic cosmic-ray anisotropy during the Forbush decrease starting 2013 April 13. *Astrophys. J.* 2018, vol. 852, no. 2, L26. DOI: [10.3847/2041-8213/aaa407](https://doi.org/10.3847/2041-8213/aaa407).

URL: <https://omniweb.gsfc.nasa.gov/form/dx1.html> (accessed March 1, 2023).

URL: <http://spaceweather.izmiran.ru/eng/dbs.html> (accessed March 1, 2023).

URL: <http://www.srl.caltech.edu/ACE/ASC/DATA/level3/icmetable2.htm> (accessed March 1, 2023).

URL: <https://www.nmdb.eu> (accessed March 1, 2023).

This paper is based on material presented at the 18th Annual Conference on Plasma Physics in the Solar System, February 6–10, 2023, IKI RAS, Moscow.

Original Russian version: Petukhova A.S., Petukhov I.S., Petukhov S.I., Gotovtsev I.S., published in *Solnechno-zemnaya fizika*. 2023. Vol. 9. Iss. 2. P. 94–100. DOI: [10.12737/szf-92202311](https://doi.org/10.12737/szf-92202311). © 2023 INFRA-M Academic Publishing House (Nauchno-Izdatelskii Tsentr INFRA-M)

How to cite this article

Petukhova A.S., Petukhov I.S., Petukhov S.I., Gotovtsev I.S. Peculiarities of medium parameter dynamics and cosmic ray density in strong Forbush decreases associated with magnetic clouds. *Solar-Terrestrial Physics*. 2023. Vol. 9. Iss. 2. P. 88–93. DOI: [10.12737/stp-92202311](https://doi.org/10.12737/stp-92202311).